WILEY-VCH

DOI: 10.1002/((please add manuscript number))
Article type: Communication

Behaviour of *in situ* cross-linked hydrogels with rapid gelation kinetics on contact with physiological fluids

*[1]Ramadan Diryak, [2]Dr. Vassilis Kontogiorgos, [1]Dr Muhammad U. Ghori [4]Dr. Paul Bills, [4]Ahmed Tawfik, [3]Prof. Gordon A. Morris, [1]Dr. Alan M Smith**

[1] Department of Pharmacy, University of Huddersfield, Queensgate, Huddersfield, HD1 3DH
[2] Department of Biological Sciences, University of Huddersfield, Queensgate, Huddersfield, HD1 3DH
[3] Department of Chemical Sciences, University of Huddersfield, Queensgate, Huddersfield, HD1 3DH
[4] EPSRC Future Metrology Hub, University of Huddersfield, Queensgate, Huddersfield HD1 3DH, UK

*author to which all correspondence should be addressed: a.m.smith@hud.ac.uk

Keywords: gelation, biopolymers, physiologically responsive, rheology, delivery systems

Among many polymeric drug or cell delivery systems *in situ* gelling polymers have shown particular promise. *In situ* gelling systems are polymeric formulations that are in the liquid state prior to administration and then undergo a rapid gelation reaction under physiological conditions with the rate of gelation and subsequent gel strength often critical to their function. The sol-gel transition of *in situ* gelling polymers depends on one or a combination of different environmental triggers such as changes in pH, temperature, and the presence of ions, that all influence polymer-polymer and polymer-solvent interactions. [1] The development of *in situ* gel systems has received considerable attention over the past 25 years [2, 3, 4, 5] sparked by the numerous advantages of such delivery systems. These include, ease and reduced frequency of administration leading to improved patient compliance. [6]

There are many polymers natural and synthetic (gellan gum, alginate acid, xyloglucan, pectin, chitosan, poly(DL-lactic acid), poly(DL-lactide-co-glycolide) and poly-caprolactone) that undergo physiological *in situ* gelation and therefore could potentially be used for drug delivery or cell delivery *via* multiple administration routes. [1] Xyloglucan, for example, forms thermally reversible gels on warming to body temperature. [7] Some other polysaccharides are pH-dependent such as carbopol (polyacrylic acid based), which undergo sol-gel transition at neutral pH while other polymers such as low acyl gellan gum, alginate and low methoyl pectin undergo sol-gel transitions at acidic pH (~pH 3.5) [1] or in the presence of physiological concentrations of cations. [8, 9] Thermally gelling events are relatively easy to measure using commercially available rheometers fitted with a Peltier plate to accurately control the temperature of the sample. Measuring rapid gelling events that occur on contact with ions or changes in pH, however, are more much challenging to measure in real time using conventional rheological apparatus. The procedure adopted in many investigations of *in situ* gelation behaviour involves loading the gelling sample into dialysis tubing and immersing into a solution of the crosslinker for various periods of time before being removed and sliced to an

appropriate size for rheological testing. [10, 11] Other methods include, pouring the gelling polymer into tissue culture plates containing filter paper soaked with the crosslinker. The sample is then incubated for the required gelation time and then loaded onto a rheometer to be measured. [12, 13] Neither of these methods, however, offers suitable experimental simulation of rapid gelation behaviour in physiological conditions. Recently in our laboratories we have demonstrated the experimental monitoring of the external gelation of alginate by modifying a commercially available rheometer. [14] In this paper, we have explored the potential of this modification, as an experimental simulation of *in situ* gelation on exposure to simulated physiological environments using gellan gum as a model *in situ* gelling delivery system **(Figure 1)**. Low acyl gellan was chosen due to its rapid gelation kinetics and sensitivity to multiple cations found in different physiological fluids.

Gellan gum forms transparent aqueous gels through a molecular ordering process in the presence of cations to form a three dimensional network. Unlike many other ionotropically gelling polysaccharides gellan forms gels with both group I and group II metal ions (and H^+) at physiologically relevant concentrations. The strength of the gels produced, however, depend on the concentration of gellan [9] and the concentration and species of the crosslinking ions (the concentrations required to induce gelation are typically in the region of 5 mM Ca^{2+} and Mg^{2+}, or 50 mM for Na^+ and K^+). This gelation behaviour of gellan is currently exploited as an ingredient in ophthalmic formulations of timolol maleate which gels *in situ* on exposure to the cations in lacrimal fluid, thus, increasing the medication retention time in the eye. [15] Furthermore, several other *in situ* gelling delivery systems prepared from gellan have been explored targeting a range of delivery sites that include gastric, nasal and wounds. [16, 17, 18, 19] To date, however, real time rheological behaviour of the gelation event on contact with these physiological fluids have yet to be suitably characterised. Therefore, the development of a suitable model to monitor the sol-gel transition of such materials in a simulated physiological

environment is important from a drug or cell delivery perspective, as gelation behaviour will ultimately impact on retention at the delivery site and subsequent bioavailability.

Here, samples of gellan gum were prepared at concentrations of 0.25%, 0.5% 0.75% and 1% w/w then loaded onto a modified rheometer and small deformation oscillatory measurements of storage (G′) and loss (G″) modulus were taken as a function of time. After 5 min (to allow the residual stress of loading to dissipate) the samples were exposed *in situ* to a range of simulated physiological fluids that included saliva (SF), wound fluid (WF), lacrimal fluid (LF) and gastric fluid (GF) **(Figure 1)** and measurements were continued for a further 20 min. A rapid growth in G′ occurred almost instantaneously as the physiological fluids were added corresponding to the onset of gelation due to the ions present in the physiological fluids (**Figure 2A)**. Addition of artificial SF gave the lowest gel strength with the GF producing the strongest gels. This is attributed to H^+ having a much greater affinity to the gellan than that of the group I and II metal ions in the other fluids. Indeed, when studying of the effect of monovalent and divalent cations Grasdalen and Smidsrød (1987) described HCl as the most potent gel-former for gellan. [20] This was evident across all the concentrations tested (Figure S1). Furthermore, stiffness of the gels formed following 20 min exposure were shown to be concentration-dependent for all the fluids tested with the GF forming the stiffest and the SF the weakest gels with the LF and WF producing gels that were not significantly different from each other ($p<0.05$) **(Figure 2B)**.

To investigate the kinetics of the *in situ* sol-gel transitions of gellan in the different physiological fluids the gelation curves were fitted to the Gompertz model **(Equation 1)** [21] and the rate constant and maximum growth rates were calculated **(Equation 2)**. The gelation curves correspond well to the sigmoidal shape of the Gompertz function and has previously been used to model biopolymer gelation. [22] Rate constants were found to follow zero-order kinetics **(Figure 2C)** in each of the physiological fluids revealing concentration independent

gelling behaviour. Gelation of gellan when applied as *in situ* gelling systems relies on the diffusion of the surrounding cations into the sample. As these cations are available within the physiological fluids in excess, it is plausible to expect concentration independent gelation behaviour with only final gel strength dependent on polymer concentration. Consequently, storage modulus (G′) reaches its pseudo-plateau value at the same time, irrespective of gellan concentration. Therefore, to achieve maximum stiffness requires appreciably different maximum growth rates, as final gel strength varies with concentration **(Figure 2B).** For that reason, growth kinetics, at the inflection point of the gelation curves, were plotted confirming concentration dependent maximum growth rates **(Figure 2D).** This is important as rate of gel network growth provides an insight into microstructure development which has important technological consequences in the application of such materials. It should be noted that temperature also influences gelation kinetics and therefore the absolute rate constant values of the gellan gelation should be viewed relative to the physiological environment of application. Moreover, as gelation behavior is dependent on diffusion of cations into the sample, then the diffusion coefficient of the different cation species could also influence gelation along with concentration and species affinity for gellan crosslinking. In addition, as quantification of the concentrations of ions diffused into the sample is unknown there is a high likelihood that the samples are more crosslinked closer to the surface, as previously been reported. [11]

Interestingly, the stiffness of the gels formed by 1% gellan in SF and 0.75% gellan in LF or WF was the same stiffness as the gels formed by 0.25% gellan exposed to GF **(Figure 3F)**. Although the stiffness of these gels (1% in SF, 0.75% LF and WF and 0.25% GF) were essentially the same following 20 min exposure to the particular physiological fluid, the calculated gelation rate constants where different (~2.2, 0.5, 0.2, 0.1 s^{-1} in GF, LF, WF and SF respectively). It was anticipated that the microstructure of these gels would be different as microstructure development is dependent on polymer concentration and gelation kinetics. [22, 23] In particular, gels that form rapidly tend to have a microstructure with larger pore sizes and

regions of densely packed polymer when compared with gels that develop over a longer period of time. [21] Furthermore, less densely packed structures are prone to molecular rearrangements resulting in microstructural collapse and subsequent changes to functionality.

To investigate this further, gels were recovered from the rheometer following *in situ* gelation, freeze dried and then analysed using surface profilometry and micro-CT. The surface texture profiles revealed a more porous network **(Figure 3A)** with larger surface peaks and valleys in the GF gels (**Figure 3A**), which also had a significantly rougher surface (**Figure 3D**) when compared with the other freeze dried gels ($p < 0.001$). This is thought to be the result of the concentration difference among the samples (0.25 % GF, 0.75 % LF, 0.75 % WF and 1 % SF). When the same samples were imaged using micro-CT it was observed that the internal microstructure of the freeze dried GF gel was the most densely packed (**Figure 3C**) and in particular contrast with the gel that was formed in the SF, which appeared to have fewer dense regions. This seemed contradictory to the surface texture analysis where the GF gels were highly porous and the SF gels were relatively homogeneous (**Figure 3A)**. This can be explained however, through close examination of the rate constants which reveal that the densely packed structure observed in the GF gel was formed at the highest gelation rate (rate constant = 2.2 s^{-1}). This is due to the gelation mechanism of gellan when exposed to low pH whereby the negative repulsive electrostatic columbic interactions are rapidly quenched leading to formation of ordered junction zones manifesting as large aggregated bundles of the polymer. Indeed, Yamamoto and Cunha reported that local aggregation of the molecules in acid gelled gellan also resulted in a structure with larger pores. [25] Moreover, Bradbeer et al (2014) suggests that the rate of aggregation using direct HCl addition is expected to be much higher than the rate achieved by slower more controlled gelation process resulting in altered elasticity and strength of the overall gellan structure. [26] This can also be observed in the mechanical spectra of the different gels (Figure S2), where the GF gels appear stronger (higher modulus values) but more brittle (failure at high frequencies) than the gels formed in the other fluids. It is likely that the

more densely aggregated bundles of the GF gels would lead to a more heterogeneous bulk structure with more surface undulations as observed in the surface profiles (**Figure 3A**) The SF gels on the other hand had a smoother surface texture due to a higher polymer concentration and a relatively heterogeneous network structure that was slowly developed (rate constant = 0.1 s^{-1}) resulting in smaller junction zones. The lower porosity measured in the SF gels **(Figure 3E)** however, are not evident in the micro CT images with relatively few areas of densely packed polymer chains and large areas that appear as voids. This is due to the resolution of the micro CT imaging which is unable to resolve the fine mesh of the gel network and only showing areas of densely packed polymer (**Figure 3C**). The relative low concentration of crosslinking ions in the SF generates a less aggregated system. This has been shown previously by Milas and Rinaudo (1996) who reported a threshold in concentrations required for the association of gellan helices into aggregates as 20 mM for K^+ and 45 mM for Na^+, [27] which is consistent with the order of effectiveness reported by Grasdalen and Smidsrød (1987) for gelation of gellan with Group I cations. [20] Taking this into account, the concentration of these species in the SF used to make the gels were 19 mM and 5.8 mM for K^+ and Na^+ respectively. Therefore, any strong bundles of aggregates would be minimal as was observed in the micro CT images of the SF gel. The microstructure of the gels formed in the WF and the LF appeared to be similar with some areas of dense aggregation of the gellan chains. This is a result of the ion content in both fluids being similar in species and in a concentration above the thresholds for aggregation of gellan helices (145 mM Na^+ and 20 mM K^+).

It should be mentioned that freeze dried gel structures are affected by ice crystal formation during the freezing step. However, the freezing step was performed in liquid nitrogen (boiling point -196 °C) to achieve glassy ice formation (-137 °C) and minimise ice crystal formation. It is however, possible that the microstructure could have been affected by the freezing process as softer gels are perhaps more likely to accommodate amorphous ice, as the gel network is more compliant, resulting in larger pores after freeze-drying. [28] However, the

gels produced from 1% gellan in SF, 0.75% gellan in LF or WF and 0.25% gel exposed to GF, all had very similar stiffness **(Figure 3F)**. It is proposed that this was due to the strength of the junctions being greater (but fewer) in the large dense bundles of gellan chains formed in the GF in contrast to numerous, smaller loosely associated junctions in the SF gels which ultimately result in similar modulus values of the bulk gel **(Figure 3G)**. What is apparent however, is that there is a complex interplay between polymer concentration, gel forming ion species and subsequent gelation kinetics that result in very different microstructures which will ultimately impact on functionality. Understanding these processes can lead to having a more informed approach when designing *in situ* gelling delivery systems for different target sites in the body.

In summary, we have presented a methodology that facilitates analysis of gelation kinetics *in situ* that represents a major step forward in the characterization of *in situ* gelling systems, as it permits the delivery of extraneous crosslinkers and real time analysis of materials with extremely rapid gelation kinetics. This provides important information, not only on predicting the speed and strength of the sol-gel transition at specific physiological sites, but also indirectly delivers an insight into microstructural development. Although it is known that the gelation gellan gum varies with different concentrations and species of cations, [9] this work reports for the first time that the microstructure of gellan gum hydrogels formed *in situ* depends on the physiological environment to which it is administered. Moreover, this method could be generalised and applied to other ionotropic gelling materials. The physiologically realistic manner of measuring real-time rheological behaviour demonstrated in this study, could be used as an effective tool during the design of *in situ* gelling systems for pharmaceutical, food and biomedical applications where tailored gelation kinetics and tuned microstructure are required to optimise functionality.

Experimental Section

Preparation of gellan solution

Gellan solutions were prepared by dissolving low acyl gellan gum (CP Kelco, UK) in deionised water at 85 °C (to produce solutions 0.25%, 0.5%, 0.75% and 1% w/w final polymer concentration). The samples where then allowed to quiescently cool to room temperature prior to use.

Preparation of physiological fluids

Artificial GF was prepared from a 1M HCl stock solution (Sigma Aldrich, UK) which was diluted tenfold with deionised water. The pH of the resulting 0.1M HCl solution was adjusted to 2 using 0.1 M NaOH. Artificial SF was prepared following the formulation reported by Parker et al (1999) with the pH of solution was adjusted accordingly to pH 6.7. [29] The composition of simulated LF was adopted from a lacrimal fluid analysis [30] and pH adjusted to 7.4 Simulated WF was prepared according to the formulation described by Bowler et al., 2012. [31] The pH of the formulated simulated WF was adjusted accordingly to pH 7.4.

Experimental simulation of in situ gelation

The experimental setup used a Malvern Gemini Nano HR rheometer with a modified lower plate **(Figure 1)**. Briefly, a petri dish containing a filter paper was securely attached to the lower plate of the rheometer. A semi permeable membrane (MWCO 14,000 g/mol) which had previously been hydrated in deionised water was placed on top of the filter paper to prevent the sample being imbibed by the filter paper. The gap was zeroed and gellan samples were then loaded onto the semi permeable membrane and silicone oil was applied around the periphery of the geometry to prevent evaporation. Small deformation oscillatory measurements of storage modulus (G′) were then performed as a function of time at 0.5% strain and a frequency of 10 rad s^{-1} using a 55 mm diameter parallel plate geometry with 1 mm gap. Measurements were performed at 32 °C for gellan with WF to represent skin temperature and 37 °C for the other types of physiological fluids. Following 5 min of measurements, 10 mL of physiological fluid was added to the filter paper on the lower plate to trigger gelation. Control samples gellan were

measured in the same way with deionized water added to the filter paper in place of the physiological fluids. All measurements were performed within the linear viscoelastic region previously determined from amplitude sweeps. All measurements were performed in triplicate and average curves plotted.

Kinetic modelling

The evolution of storage modulus with time is described by the empirical Gompertz double exponential growth model:

$$\log G'(t) = \log G'_{\infty}\ e^{-e^{(b-ct)}} \qquad (1)$$

where log G′ (t) is storage modulus as a function of time and log G′$_{\infty}$ is the value of log G′ at the plateau region of the curve, constant *c* represents the scaling of storage modulus along the *y*-axis (rate constant) and *b* is a positive parameter equal to c^*t_i with t_i corresponding to the time at the inflection point. In this model the maximum growth rate is given by:

$$\frac{c \log G'_{\infty}}{e} \qquad (2)$$

The growth rate values were estimated and plotted *vs* concentration for all samples. Non-linear regression fitting was performed using GraphPad Prism v.6 (GraphPad software, San Diego, USA).

Profilometry

Polymer network and surface texture of freeze dried gels were examined using Talysurf CCI 3000 optical 3D surface profiler which have the capability of measuring over one million data points in less than 10 s with a resolution of 0.01 nm. Briefly, a sample of freeze dried gel (1 × 1 cm) was fixed on a stainless steel wafer (3 × 3 cm) using double sided transparent tape. The

uniform gel fixation process was confirmed using an optical microscope equipped with 5.0 MP camera (Supereyes®, UK). The sample was then placed under the microscopic arm of the profiler in a cleanroom environment and 800 × 800 μm regions were scanned to obtain reliable statistics. The height variation in the resulting topography maps is represented by a colour scheme and the topographical information can be reliably inferred from the given colour scheme. Surface roughness was determined using Surfstand® Software. [32, 33] Moreover, using ImageJ (version 1.47*i*) the images were binarized using the Sauvola method [34] and porosity of freeze dried gels was determined using BoneJ particle analyser plug-in. [35]

Micro Computed Tomography (μ-CT)

Prior to imaging the samples were fixed in pipette tips and allowed to stabilise at room temperature for a period of 24 h. Samples were imaged using a Nikon XTH 225 μ-CT system (Nikon Metrology, UK) with a tungsten reflection X-ray target. Datasets were acquired at 80 kV, 3.5 W with a resulting voxel size of 9 μm. Each dataset consisted of 1583 individual X-ray projections which were then reconstructed using CT Pro (Nikon Metrology, UK), and standard algorithms were used for noise reduction and beam hardening compensation. Compensation was carried out using two horizontal slices at opposite extremities of each dataset to take into account any shading gradient across the image. Image exposure was set at 500 ms and a 0.5 mm Cu filter was used to remove low energy X-rays from reaching the sample. The acquired data processing, surface determination process and defect analysis was performed using VGStudio Max software (Volume Graphics GmbH, Germany). Data relating to the plastic pipette and surrounding air was removed from the analysis by demarcation of the dataset shading histogram repeatedly between datasets. Cross-sections were then taken at pre-determined points through each sample such that qualitative comparison could be performed.

Supporting Information

Supporting Information is available from the Wiley Online Library or from the author.

Acknowledgements
The authors gratefully acknowledge the Engineering and Physical Sciences Research Council (EPSRC) funding of the EPSRC Centre for Innovative Manufacturing in Advanced Metrology (Grant Ref: EP/I033424/1).

Received: ((will be filled in by the editorial staff))
Revised: ((will be filled in by the editorial staff))
Published online: ((will be filled in by the editorial staff))

References

[1] M. Madan, A. Bajaj, S. Lewis, N. Udupa, J. A. Baig, *Indian J. Pharm. Sci.* **2009**, 71, 242.
[2] N. Peppas, R. Langer, Science 1994, **263**, 1715.
[3] H. Almeida, M. H. Amaral, P. Lobão, J. M. Lobo. Drug Discov. Today 2014, 19, 400-412
[4] L. Klouda, Eur. J. Pharm. Biopharm 2015, 97, 338-349
[5] P. L. Destruel, N. Zeng, M. Maury, N. Mignet, V. Boudy. Drug Discov. Today 2017, 22, 638-651
[6] N. HB, S. Bakliwal, S. Pawar, *I. J. PharmTech. Res*. **2010** 2, 1398
[7] S. Miyazaki, S. Suzuki, N. Kawasaki, K. Endo, A. Takahashi, D. Attwood, *Int. J. Pharm.* **2001**, 229, 29.
[8] G. Sworn, G. Sanderson, W. Gibson, *Food Hydrocoll.* **1995**, 9, 265.
[9] E. R. Morris, K. Nishinari, M. Rinaudo, *Food Hydrocoll.* **2012**, 28, 373.
[10] W. Kubo, S. Miyazaki, D. Attwood, *Int. J. Pharm.* **2003**, 258, 55.
[11] S. Miyazaki, N. Kawasaki, W. Kubo, K. Endo, D. Attwood, *Int. J. Pharm.* **2001**, 220, 161.
[12] N. C. Hunt, A. M. Smith, U. Gbureck, R. M. Shelton, L. M. Grover, *Acta Biomater.* **2010**, 6, 3649
[13] S. H. Jahromi, L. M. Grover, J. Z. Paxton, A. M. Smith, *J. Mech. Behav. Biomed. Mater.* **2011**, 4, 1157
[14] M. Mahdi, R. Diryak, V. Kontogiorgos, G. Morris, A. M. Smith, *Food Hydrocoll.* **2016**, 55, 77.
[15] A. Rozier, C. Mazuel, J. Grove, B. Plazonnet, *Int. J. Pharm.* **1989,** 57**,** 163.
[16] P. Rajinikanth, B. Mishra, *J. Control. Release* **2008**, 125, 33.
[17] M. H. Mahdi, B. R. Conway, A. M. Smith, *Int. J. Pharm.* **2014**, 475, 335.
[18] M. H. Mahdi, B. R. Conway, A. M. Smith, *Int. J. Pharm.* **2015**, 488, 12.
[19] C. Cencetti, D. Bellini, A. Pavesio, D. Senigaglia, C. Passariello, A. Virga, P. Matricardi, *Carbohydr. Polym.* **2012**, 90, 1362.
[20] H. Grasdalen, O. Smidsrød, *Carbohydr. Polym.* **1987**, 7, 371.
[21] C. P. Winsor, *Proc. Natl. Acad. Sci.* **1932**, 18, 1.
[22] V. Kontogiorgos, H, Vaikousi, A. Lazaridou, C. G. Biliaderis *Colloids Surf. B* **2006**, 49, 145
[23] T. R. Hoare, D. S. Kohane, *Polymer* **2008**, 49, 1993.
[24] M. Salzano de Luna, R. Altobelli, L. Gioiella, R. Castaldo, G. Scherillo, G. Filippone, *J. Polym. Sci. Part B Polym. Phys.* **2017**, 24436
[25] F. Yamamoto, R. Cunha, *Carbohydr. Polym.* **2007**, 68, 517.
[26] J. F. Bradbeer, R. Hancocks, F. Spyropoulos, I. T. Norton, *Food Hydrocoll.* **2014**, 35, 522.
[27] M. Milas, M. Rinaudo, *Carbohydr. Polym.* **1996**, 30, 177.
[28] G. W. Scherer, *J. Am. Ceram. Soc.* **1990**, 73, 3.

[29] S. Parker, D. Martin, M. Braden, Biomaterials **1999**, 20, 55.
[30] M. Stjernschantz J. and Astin, in *Biopharmaceutics of Ocular Drug Delivery*, CRC Press, Boca Raton **1993**, 1.
[31] P. G. Bowler, S. Welsby, V. Towers, R. Booth, A. Hogarth, V. Rowlands, A. Joseph, S. A. Jones, *Int. Wound. J.* **2012**, 9, 387.
[32] L. Blunt, X. Jiang, *Advanced techniques for assessment surface topography: development of a basis for 3D surface texture standards" surfstand"*, Elsevier, **2003**.
[33] M. U. Ghori, M. A. Mohammad, S. R. S. Rudrangi, L. T. Fleming, H. A. Merchant, A. M. Smith, B. R. Conway, *Food Hydrocoll.* **2017**, 71, 311
[34] J. Sauvola, M. Pietikäinen, *Pattern Recognit.* **2000**, 33, 225.
[35] M. Doube, M. M. Kłosowski, I. Arganda-Carreras, F. P. Cordelières, R. P. Dougherty, J. S. Jackson, B. Schmid, J. R. Hutchinson, S. J. Shefelbine, *Bone* **2010**, 47, 1076.

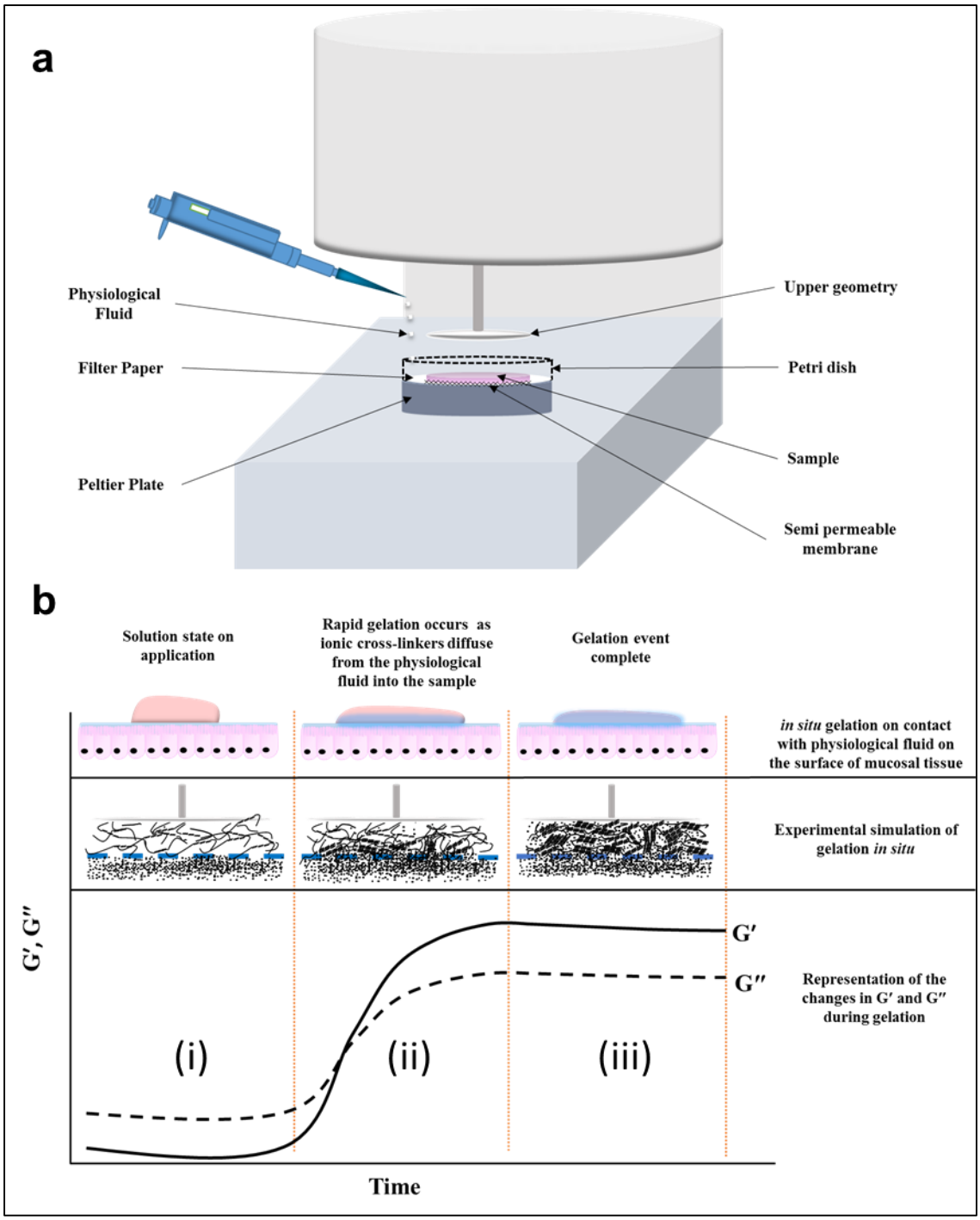

Figure 1. a) Schematic diagram showing the experimental rheometer setup for the *in situ* gelation measurements and b) illustration of how the experimental model simulates the gelation process encountered on the surface of mucosal tissue. Section (i) the material in the solution state on application with G″ > G′, section (ii) onset of gelation as crosslinking ion diffuse into the gelling material corresponding to an increase in G′ and G″ with moduli crossing over at the gelation point and section (iii) plateau region occurring when gelation is complete corresponding to G′ > G″ and no further increase in moduli.

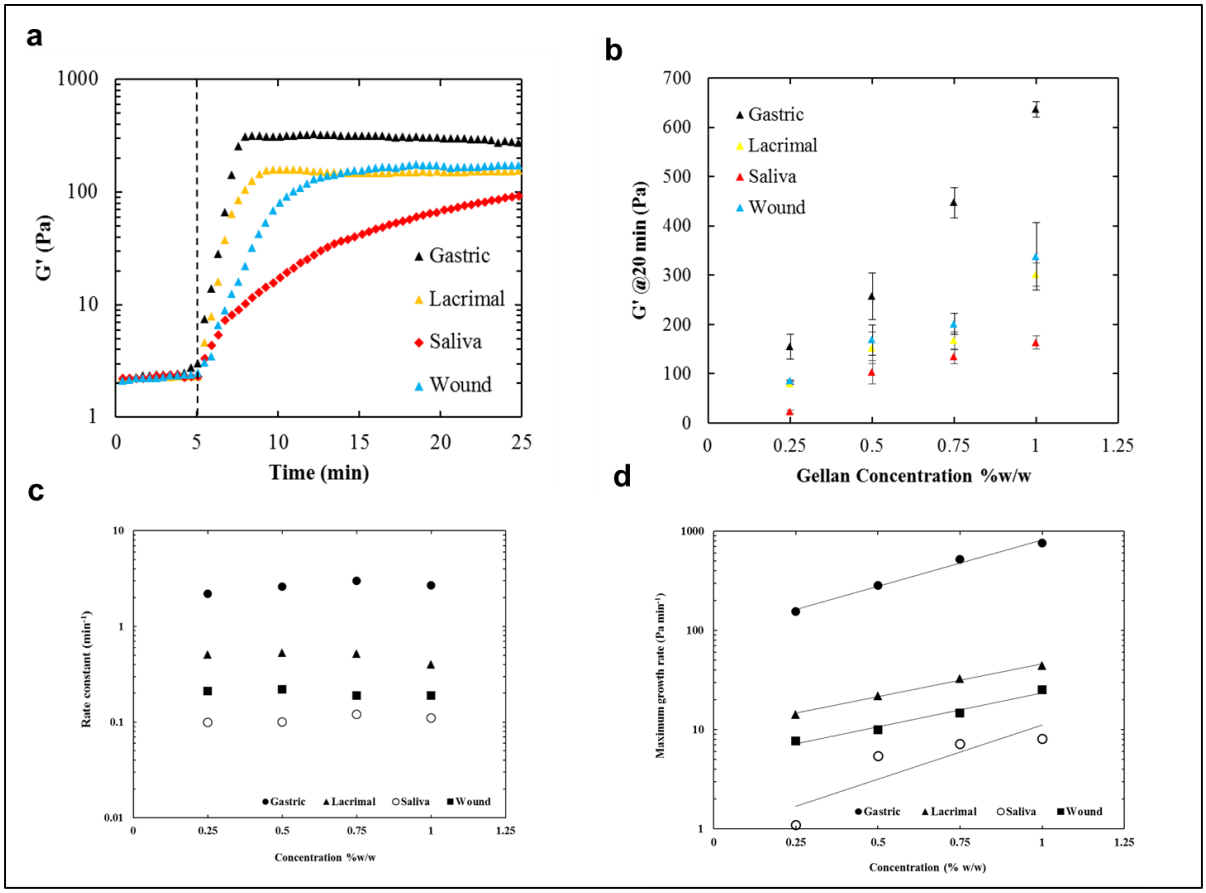

Figure 2. a) Typical *in situ* gelation curves showing changes in storage modulus as a function of time for gellan gum at 0.5% w/w when exposed to GF, LF, SF and WF. The vertical dashed line denotes the time at which the physiological fluids were added. b) The storage modulus following 20 minutes *in situ* exposure to the fluids highlighting the concentration dependence of gel stiffness and the variations in stiffness between the different physiological fluids tested. c) Gelation curves were fitted to the Gompertz model which revealed zero-order kinetics in all physiological fluids but were significantly different between the different fluids ($P<0.05$) whereas d) Maximum growth rate was concentration dependent in all physiological fluids.

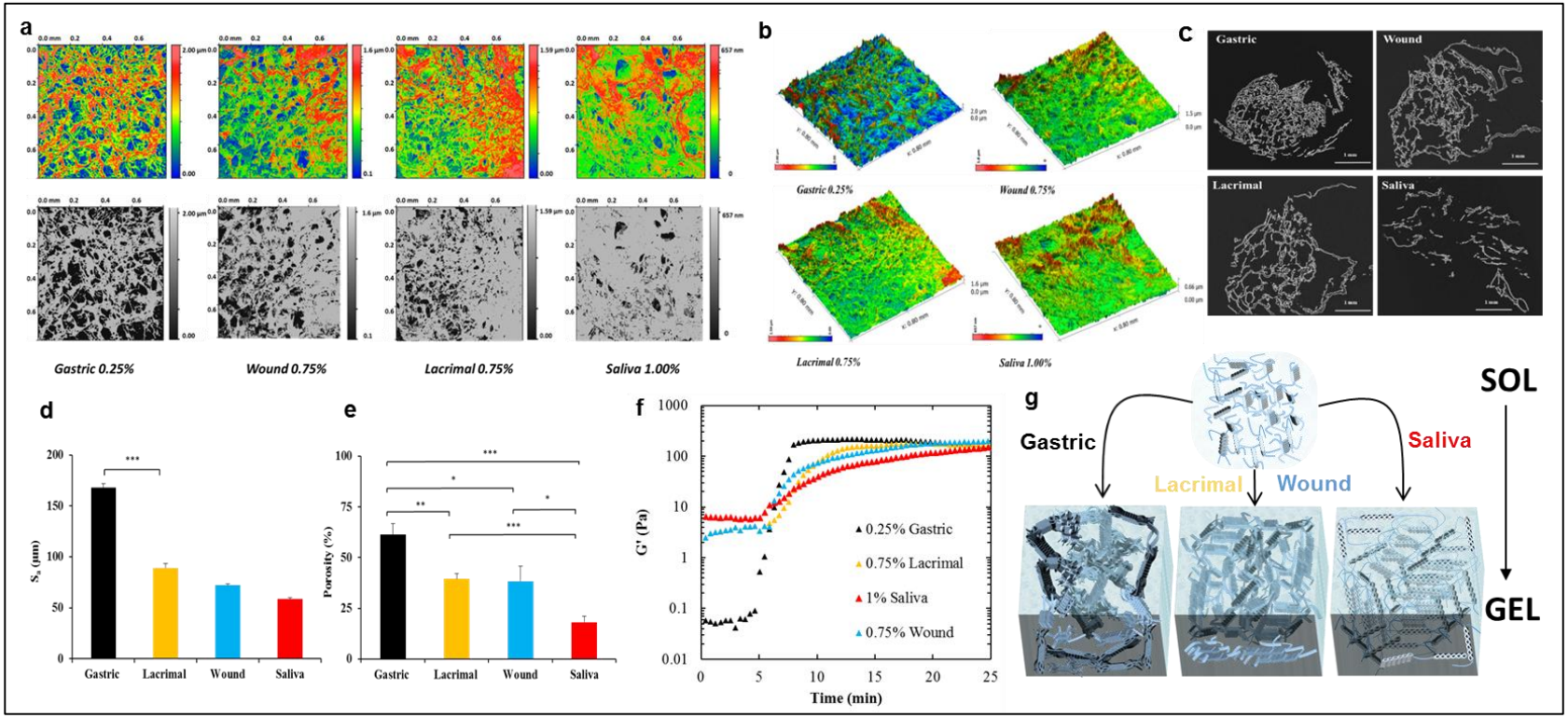

Figure 3. a) Profilometry images of the freeze dried samples of 0.25% gellan in GF, 0.75% gellan in LF and in WF, 1% gellan in SF (top) and corresponding processed images after binarization process (bottom). b) 3D isometric surface images of the freeze dried samples of 0.25% gellan in GF, 0.75% gellan in LF and WF, 1% gellan in SF showing valleys and peaks on the surface with the deepest pores represented in blue. c) Micro CT images showing regions of densely packed polymer in freeze dried 0.25% gellan gelled in GF, 0.75% gellan gelled in LF, 0.75% gellan gelled in WF and 1% gellan gelled in SF. d) 3D surface texture parameters determined using Surfstand® software showing arithmetical average of surface roughness of the freeze dried gels. e) Numerical values of overall porosity of freeze dried gels. f) *in situ* gelation curves for the imaged gels prior to freeze drying, showing changes in storage modulus as a function of time. Curves highlight the similar values of stiffness achieved by 1% gellan in SF, 0.75% gellan in LF or WF and 0.25% gel exposed to GF. g) Schematic diagram of the proposed microstructural differences achieving similar modulus values in different gellan concentrations when gelled with different physiological fluids. *In situ* gelation in GF causes the formation of densely aggregated bundles which is in contrast to the gels formed in SF which forms a more homogeneous less densely packed microstructure. (* = $p < 0.05$, ** = $p < 0.01$, *** = $p < 0.001$)

Keyword: gelation, biopolymers, physiologically responsive, rheology, delivery system

Authors: Ramadan Diryak, Dr. Vassilis Kontogiorgos, Dr. Muhammad U. Ghori, Dr. Paul Bills, Ahmed Tawfik, Prof. Gordon A. Morris, Dr. Alan M Smith*

Title: Behaviour of *in situ* cross-linked hydrogels with rapid gelation kinetics on contact with physiological fluids

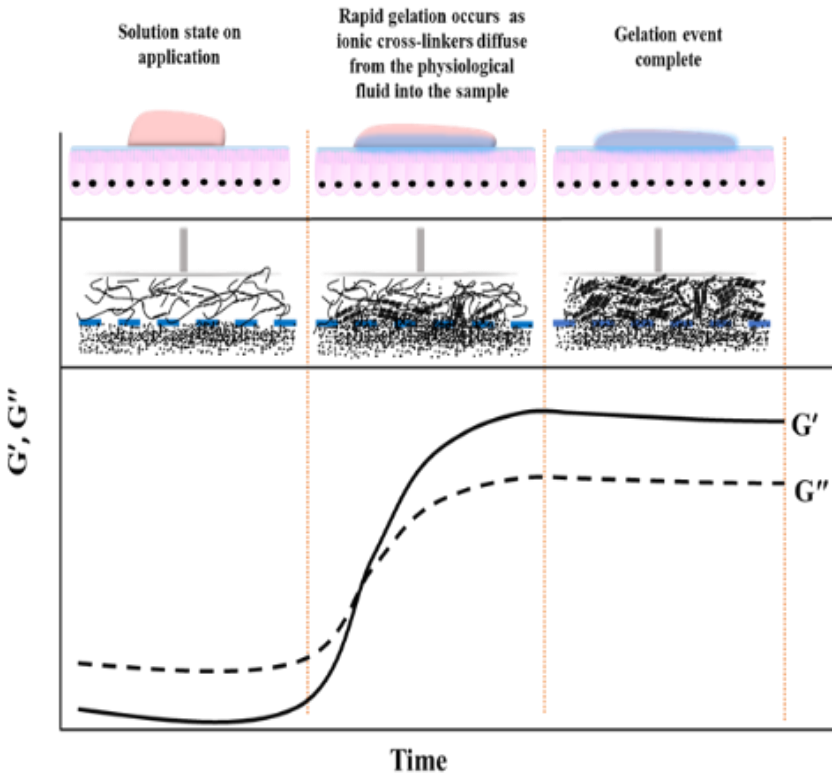

Behaviour of in situ cross-linked hydrogels with extremely rapid gelation kinetics on contact with physiological fluids. The power of this method is demonstrated by measuring in real-time, the rapid gelation kinetics and gel strength of gellan gum exposed to gastric, lacrimal, saliva and wound fluid, highlighting potential use in the intelligent design of *in situ* gelling delivery systems.